Heat-treated virus inactivation rate depends strongly on treatment procedure

Amandine Gamble[1,*], Robert J. Fischer[2,*], Dylan H. Morris[3], Kwe Claude Yinda[2], Vincent J. Munster[2], and James O. Lloyd-Smith[1]

[1] *Department of Ecology & Evolutionary Biology, University of California, Los Angeles, CA, USA*
[2] *Laboratory of Virology, National Institute of Allergy and Infectious Diseases, Hamilton, MT, USA*
[3] *Department of Ecology & Evolutionary Biology, Princeton University, NJ, USA*
[*] *these authors contributed equally*

August 10, 2020

Abstract

Decontamination of objects and surfaces can limit transmission of infectious agents via fomites or biological samples. It is required for the safe re-use of potentially contaminated personal protective equipment and medical and laboratory equipment. Heat treatment is widely used for the inactivation of various infectious agents, notably viruses. We show that for liquid specimens (here suspension of SARS-CoV-2 in cell culture medium), virus inactivation rate under heat treatment at 70°C can vary by almost two orders of magnitude depending on the treatment procedure, from a half-life of 0.86 min (95% credible interval: [0.09, 1.77]) in closed vials in a heat block to 37.0 min ([12.65, 869.82]) in uncovered plates in a dry oven. These findings suggest a critical role of evaporation in virus inactivation using dry heat. Placing samples in open or uncovered containers may dramatically reduce the speed and efficacy of heat treatment for virus inactivation. Heating procedures must be carefully specified when reporting experimental studies to facilitate result interpretation and reproducibility, and carefully considered when designing decontamination guidelines.

1. Introduction

The COVID-19 pandemic has led to millions of infections worldwide, but the relative contribution of different modes of transmission of its causative agent, SARS-CoV-2, remains elusive. Transmission is thought to occur primarily via large respiratory droplets and close contact, but transmission via aerosols and fomites has also been suggested [1–4]. In this context, and considering the non-negligible environmental stability of SARS-CoV-2 on different surfaces [5, 6], there is a need for rapid and effective decontamination methods. Clearly, decontamination is a concern for all other infectious agents as well.

Heat is widely used for the inactivation of various infectious agents, notably viruses [7]. It is thought to inactivate viruses mainly by denaturing the secondary structures of proteins and

other molecules, resulting in impaired functions [8]. It is used for the decontamination of various materials, such as personal protective equipment (PPE), examination and surgery tools, culture and transportation media, or biological samples [9–12]. Regarding SARS-CoV-2 in particular, moist heat is advised by the United States Centers for Disease Control and Prevention as a virus inactivation method [13].

In this context, several studies have tested the effectiveness of heat to inactivate coronaviruses on various household surfaces, PPE, culture and transportation media, or blood products [11, 14–19]. The same type of procedures are used for many other viruses such as influenza viruses, hepatitis viruses, parvoviruses and human immunodeficiency viruses [20–23]. Ways to apply heat treatments vary, notably settings can use dry versus moist heat and allow different levels of heat transfer (e.g., oven versus heat block, the latter theoretically allowing a higher heat transfer) and different levels of evaporation (e.g., samples in closed vials versus in open plates, two containers classically used in laboratories). Studies often do not report detailed procedures; this may make it difficult to interpret and replicate findings or to translate them into safe guidelines if inactivation rates differ by procedure.

Here, we assess the impact of treatment procedure on SARS-CoV-2 inactivation by heat. We studied dry heat treatment applied to a liquid specimen (virus suspension in cell culture medium), keeping temperature constant (at 70°C) but allowing different degrees of heat transfer (using a dry oven or a heat block) and evaporation (placing samples in closed vials, covered plates or uncovered plates). We then compared the inactivation rates and half-lives of SARS-CoV-2 under different procedures.

2. Material and Methods

(a) Laboratory experiments

We used the SARS-CoV-2 strain HCoV-19 nCoV-WA1-2020 (MN985325.1) [24] for all our experiments. We prepared a solution of SARS-CoV-2 in Dulbecco's Modified Eagle Medium (DMEM) cell culture medium (Sigma-Aldrich). We applied four distinct heat-treatment procedures: (1) an uncovered 24-well plate, (2) a covered 24-well plate (using an unsealed plastic lid), (3) a set of closed 2 mL vials in a dry oven at 70°C, and (4) a set of closed 2 mL vials in a heat block containing water at 70°C. For each procedure, we placed samples of 1 mL of solution in plate wells or vials before heat treatment, and removed them at 10, 20, 30 and 60 min from the uncovered 24-well plate, or at 30, 60 and 90 min for the three other procedures.

For each experiment, we took a 0 min time-point measurement prior to exposing the specimens to the heat treatment. At each collection time-point, samples were transferred into a vial and frozen at -80°C until titration (or directly frozen for experiments conducted in vials). We performed three replicates for each inactivation procedure. We quantified viable virus contained in the collected by end-point titration on Vero E6 cells as described previously [11].

(b) Statistical analyses

We quantified the inactivation rate of SARS-CoV-2 in DMEM following different heat-treatment procedures by adapting a Bayesian approach described previously [11]. Briefly, we inferred virus titers from raw endpoint titration well data by modeling well infections as a Poisson single-hit process [25]. Then, we estimated the decay rates of viable virus titer following treatment using a regression model. This modeling approach allowed us to account for differences in initial virus titers (0 min time-point) across samples as well as other sources of experimental noise. The model yields posterior distributions for the viral decay rates under various treatment procedures—that is, estimates of the range of plausible values for these parameters given our data, with an estimate of the overall uncertainty [26]. We then calculated half-lives from the estimated exponential decay rates. We analyzed data obtained under different treatment procedures separately. We placed weakly informative prior distributions on mean initial virus titers and log virus half-lives. The complete model is detailed is detailed in the Supplementary Information (SI, end of this document).

We estimated virus titers and model parameters by drawing posterior samples using Stan [27], which implements a No-U-Turn Sampler (a form of Markov Chain Monte Carlo), via its R interface RStan. We report estimated titers and model parameters as the median [95% credible interval] of their posterior distribution. We assessed convergence by examining trace plots and confirming sufficient effective sample sizes and $\hat{R}$ values for all parameters. We confirmed appropriateness of prior distributions with prior predictive checks and assessed goodness of fit by plotting regression lines against estimated titers and through posterior predictive (SI, Fig. 3-5).

3. Results

The inactivation rate of SARS-CoV-2 differed sharply across the four heat-treatment procedures, leading to large differences in the time until the virus dropped below detectable levels despite comparable initial quantities of virus (mean initial titer ranging from 4.3 $[3.7, 4.7]$ to 4.8 $[4.3, 5.1]$ $\log_{10}\mathrm{TCID}_{50}/\mathrm{mL}$). We could not detect viable virus in DMEM after 30 min of treatment (the earliest time-point) in closed vials heated either in a heat block or in a dry oven; we could not detect viable virus after 90 min in covered plates (Fig. 1). In uncovered plates, we observed an reduction of viral titer in DMEM of approximately $1\log_{10}\mathrm{TCID}_{50}/\mathrm{mL}$ after 60 min.

We estimated inactivation rates from the experimental data, and converted these to half-lives to compare the four procedures. SARS-CoV-2 inactivation in DMEM was rapid in closed vials, using either a heat block or a dry oven (half-lives of 0.86 $[0.09, 1.77]$ and 1.91 $[0.10, 1.99]$ min, respectively), compared to the other treatment procedures (Fig. 2). Inactivation rate was intermediate in covered plates (half-life of 3.94 $[3.12, 5.01]$ min) and considerably slower in uncovered plates (37.04 $[12.65, 869.82]$ min).

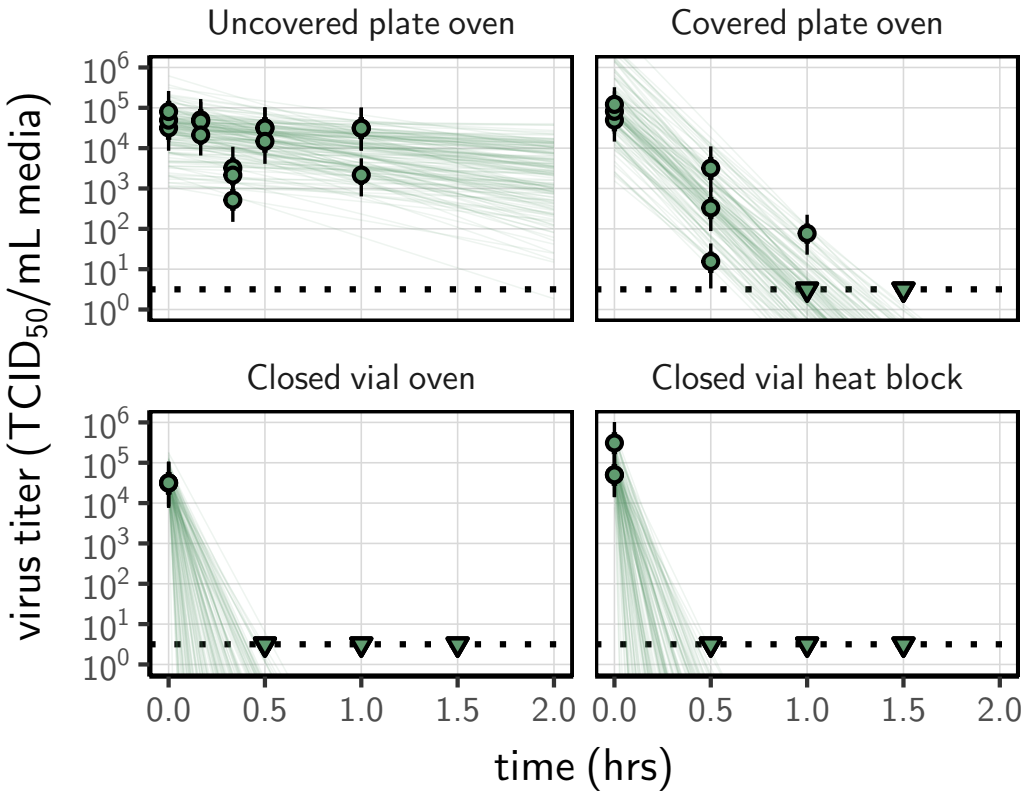

Figure 1. Inactivation of SARS-CoV-2 by heat treatment under different procedures. SARS-CoV-2 in DMEM cell culture medium was exposed to 70°C heat. Samples were placed in uncovered or covered 24-well plates, or in closed 2 mL vial before heat treatment using a dry oven or a heat block. Samples were then collected at indicted time-points during heat treatment. Viable virus titer estimated by end-point titration is shown in $TCID_{50}$/mL media on a logarithmic scale. Points show estimated titers for each collected sample; vertical bar shows a 95% credible interval. Time-points with no positive wells for any replicate are plotted as triangles at the approximate single-replicate detection limit of the assay (LOD; denoted by a black dotted line at $10^{0.5}$ $TCID_{50}$/mL media) to indicate that a range of sub-LOD values are plausible. Lines show predicted decay of virus titer over time (10 random draws per datapoint from the joint posterior distribution of the exponential decay rate, i.e. negative of the slope, and datapoint intercept, i.e. initial virus titer).

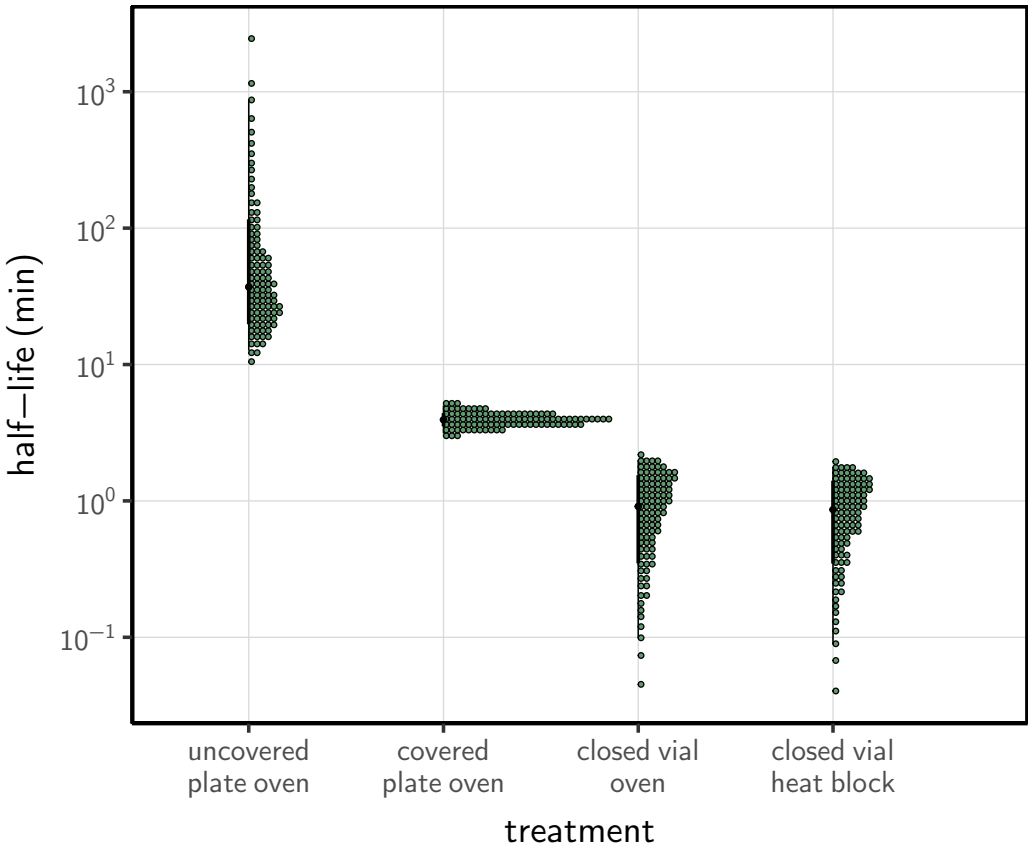

Figure 2. Half-life of SARS-CoV-2 in DMEM cell culture medium exposed to 70°C heat under different procedures. Quantile dotplots [28] of the posterior distribution for half-life of viable virus under each different heat-treatment procedure. Half-lives were calculated from the estimated exponential decay rates of virus titer (Fig. 1) and plotted on a logarithmic scale. For each distribution, the black dot shows the posterior median estimate and the black line shows the 95% credible interval.

4. Discussion

Using SARS-CoV-2 as an illustration, we demonstrate that the choice of procedure has a considerable impact on virus inactivation from liquid specimen using dry heat. In liquid specimens (here viral suspension in cell culture medium), virus half-life can vary from 0.86 min ([0.09, 1.77]) in closed vials to 37.0 min ([12.65, 869.82]) in uncovered plates treated with dry heat at 70°C. The rapid virus inactivation in closed vials subject to dry heat at 70°C agrees with previously reported results for inactivation of SARS-CoV-2 in virus transportation medium [29], SARS-CoV-1 in human serum [14], and MERS-CoV [15] and canine coronavirus in cell culture medium [18] for instance. All showed a loss of infectivity on the order of 10^{4-6} $TCID_{50}$ after 5–10 min at 65–75°C. None of these studies report sufficient details on their protocol to know which of our tested procedures corresponds most closely to their approach.

Our findings suggest a critical role for evaporation in determining the rate of virus inactivation using dry heat, bringing fundamental insights on the mechanisms by which temperature and humidity affect viral stability. There are several mechanisms by which evaporation can impact the effectiveness of heat treatments to inactivate viruses. First, evaporation can induce a local drop in temperature due to the enthalpy of vaporization of water, limiting the effect of heat itself. Second, evaporation can lead to modifications of the virion's solute environment. Salts and proteins become more concentrated as the solvent evaporates, and under certain conditions crystallization can occur [30]. Evaporation can also modify ambient pH [30]. These processes do not depend solely on temperature; factors such such as initial composition of the medium ([17, 31]) and ambient relative humidity [30] play a role. Furthermore, the effects of salinity and pH on viral infectivity are not fully characterized, and hence are difficult to predict. Better understanding the impact of temperature and humidity on viral stability is critical not only for designing efficient decontamination protocols but also for predicting viral stability under different environmental conditions—with consequences for real-world transmission [32, 33]. Heat transfer could potentially also play a role in determining the rate of virus inactivation using dry heat, but our experimental design did not allow us to explore this hypothesis since virus inactivation was fast in closed vials regardless of whether they were exposed to heat using an dry oven or a heat block.

Given the substantial effect of heat-treatment procedure on virus inactivation rates, it is critical to consider procedure closely when comparing inactivation rates between studies or producing guidelines for decontamination. In particular, our results show that protocols in open containers or uncovered surfaces lead to a much slower viral inactivation, at least in bulk medium. Hence, meta-analyses of the effect of temperature on virus inactivation integrating together data collected following different procedures can lead to false conclusions. This observation also has important implications regarding decontamination practices using heat treatment, as it highlights that inactivation rates reported by studies conducted on closed vials are likely not representative of inactivation rates one can expect using a dry oven to decontaminate a piece of equipment. As a matter of fact, the half-life of SARS-CoV-2 on stainless steel and N95 fabric treated by heat (70°C) using a dry oven, without any container susceptible to limit evaporation, has been estimated at approximately 9 and 5 min respectively [11]. These values are on the same order of magnitude as the half-life of the virus in DMEM exposed to heat treatment in a covered plate (3.94 [3.12, 5.01] min), and

considerably higher than the the half-life of the virus in DMEM exposed to heat treatment in a closed vial. Inactivation rates reported by studies conducted on closed vials should not be used to directly inform decontamination guidelines of pieces of equipment that can not be treated using the same exact procedure.

Unfortunately, many studies on heat treatment for virus inactivation do not report the exact procedures under which the samples were exposed to heat, in particular whether they were in closed, covered or uncovered containers), limiting the possibility to compare inactivation rates between studies or inform decontamination guidelines. More generally, considering all the different factors that can impact virus inactivation rate, we recommend to use decontamination procedures validated specifically for the concerned setting rather than to translate experimental studies into decontamination guidelines, especially when experimental protocols are elusive.

This study focuses exclusively on virus inactivation by heat. Other factors have been suggested to modulate virus inactivation rate in liquid specimens, including pH, salinity and protein concentration [17, 30, 34]; we consider these only implicitly, via the possible effects of evaporation. In addition, the impact of procedure is likely to differ across microbes, in particular when considering enveloped versus non-enveloped viruses, or viruses versus bacteria [30]. Finally, another critical aspect to consider is the potential impact on the integrity of the decontaminated equipment or specimen, notably for PPE and biological samples [11, 35, 36]. Any effort to translate inactivation rates (or even relative patterns) from one setting to another should thus be undertaken cautiously, accounting for these factors. Nevertheless, our findings highlight the importance of careful consideration of treatment procedures, notably regarding the degree of permitted evaporation.

Data accessibility

Code and data to reproduce the Bayesian estimation results and produce corresponding figures are available on Github: `https://github.com/dylanhmorris/heat-inactivation`

Acknowledgments

We thank Linsey C. Marr for helpful discussions. This research was supported by the Intramural Research Program of the National Institute of Allergy and Infectious Diseases (NIAID), National Institutes of Health (NIH). JOL-S and AG were supported by the Defense Advanced Research Projects Agency DARPA PREEMPT # D18AC00031 and the UCLA AIDS Institute and Charity Treks, and JOL-S was supported by the U.S. National Science Foundation (DEB-1557022), the Strategic Environmental Research and Development Program (SERDP, RC-2635) of the U.S. Department of Defense.

References

[1]S. W. X. Ong, Y. K. Tan, P. Y. Chia, T. H. Lee, O. T. Ng, M. S. Y. Wong, and K. Marimuthu, "Air, surface environmental, and personal protective equipment contamina-

tion by severe acute respiratory syndrome coronavirus 2 (sars-cov-2) from a symptomatic patient", JAMA (2020).

[2]C. Yeo, S. Kaushal, and D. Yeo, "Enteric involvement of coronaviruses: is faecal–oral transmission of sars-cov-2 possible?", The Lancet Gastroenterology & Hepatology **5**, 335–337 (2020).

[3]J. Allen and L. Marr, "Re-thinking the potential for airborne transmission of sars-cov-2", (2020).

[4]J. Cai, W. Sun, J. Huang, M. Gamber, J. Wu, and G. He, "Indirect virus transmission in cluster of covid-19 cases, wenzhou, china, 2020", Emerging Infectious Diseases **26** (2020).

[5]N. van Doremalen, T. Bushmaker, D. H. Morris, M. G. Holbrook, A. Gamble, B. N. Williamson, A. Tamin, J. L. Harcourt, N. J. Thornburg, S. I. Gerber, and et al., "Aerosol and surface stability of sars-cov-2 as compared with sars-cov-1", New England Journal of Medicine, NEJMc2004973 (2020).

[6]M. J. Matson, C. K. Yinda, S. N. Seifert, T. Bushmaker, R. J. Fischer, N. van Doremalen, J. O. Lloyd-Smith, and V. J. Munster, "Effect of environmental conditions on SARS-CoV-2 stability in human nasal mucus and sputum", Emerging Infectious Diseases **26**, in press (2020).

[7]W. Rogers, "Steam and dry heat sterilization of biomaterials and medical devices", in *Sterilisation of biomaterials and medical devices* (Elsevier, 2012), pp. 20–55.

[8]K. R. Wigginton, B. M. Pecson, T. Sigstam, F. Bosshard, and T. Kohn, "Virus inactivation mechanisms: impact of disinfectants on virus function and structural integrity", Environmental Science & Technology **46**, 12069–12078 (2012).

[9]L. Chang, Y. Yan, and L. Wang, "Coronavirus disease 2019: coronaviruses and blood safety", Transfusion Medicine Reviews (2020).

[10]A. F. Henwood, "Coronavirus disinfection in histopathology", Journal of Histotechnology (2020).

[11]R. Fischer, D. H. Morris, N. van Doremalen, S. Sarchette, J. Matson, T. Bushmaker, C. K. Yinda, S. Seifert, A. Gamble, B. Williamson, and et al., "Assessment of n95 respirator decontamination and re-use for sars-cov-2", medRxiv (2020).

[12]B. K. Heimbuch, W. H. Wallace, K. Kinney, A. E. Lumley, C.-Y. Wu, M.-H. Woo, and J. D. Wander, "A pandemic influenza preparedness study: use of energetic methods to decontaminate filtering facepiece respirators contaminated with h1n1 aerosols and droplets", American Journal of Infection Control **39**, 265–270 (2011).

[13]CDC, *Coronavirus disease 2019 (covid-19)*, Feb. 2020.

[14]M. E. R. Darnell and D. R. Taylor, "Evaluation of inactivation methods for severe acute respiratory syndrome coronavirus in noncellular blood products", Transfusion **46**, 1770–1777 (2006).

[15]I. Leclercq, C. Batéjat, A. M. Burguière, and J.-C. Manuguerra, "Heat inactivation of the middle east respiratory syndrome coronavirus", Influenza and Other Respiratory Viruses **8**, 585–586 (2014).

[16]A.-M. Pagat, R. Seux-Goepfert, C. Lutsch, V. Lecouturier, J.-F. Saluzzo, and I. C. Kusters, "Evaluation of sars-coronavirus decontamination procedures", Applied Biosafety **12**, 100–108 (2007).

[17]H. Laude, "Thermal inactivation studies of a coronavirus, transmissible gastroenteritis virus", Journal of General Virology **56**, 235–240 (1981).

[18]A. Pratelli, "Canine coronavirus inactivation with physical and chemical agents", The Veterinary Journal **177**, 71–79 (2008).

[19]S.-M. Duan, X.-S. Zhao, R.-F. Wen, J.-J. Huang, G.-H. Pi, S.-X. Zhang, J. Han, S.-L. Bi, L. Ruan, X.-P. Dong, and et al., "Stability of sars coronavirus in human specimens and environment and its sensitivity to heating and uv irradiation", Biomedical and Environmental Sciences **16**, 246–255 (2003).

[20]H. Abu-Aisha, A. Mitwalli, S. O. Huraib, J. Al-Wakeel, J. Abid, K. I. Yousif, F. Algayyar, and S. Ramia, "The effect of chemical and heat disinfection of the hemodialysis machines on the spread of hepatitis c virus infection: a prospective study", Saudi Journal of Kidney Diseases and Transplantation **6**, 174 (1995).

[21]M. Eterpi, G. McDonnell, and V. Thomas, "Disinfection efficacy against parvoviruses compared with reference viruses", Journal of Hospital Infection **73**, 64–70 (2009).

[22]E. K. Jeong, J. E. Bae, and I. S. Kim, "Inactivation of influenza a virus h1n1 by disinfection process", American Journal of Infection Control **38**, 354–360 (2010).

[23]W. H. Organization, *Guidelines on sterilization and disinfection methods effective against human immunodeficiency virus (hiv)* (1989).

[24]M. L. Holshue, C. DeBolt, S. Lindquist, K. H. Lofy, J. Wiesman, H. Bruce, C. Spitters, K. Ericson, S. Wilkerson, A. Tural, and et al., "First case of 2019 novel coronavirus in the united states", New England Journal of Medicine **382**, 929–936 (2020).

[25]C. Brownie, J. Statt, P. Bauman, G. Buczynski, K. Skjolaas, D. Lee, J. Hotta, and N. Roth, "Estimating viral titres in solutions with low viral loads", Biologicals **39**, 224–230 (2011).

[26]A. Gelman, J. B. Carlin, H. S. Stern, D. B. Dunson, A. Vehtari, and D. B. Rubin, *Bayesian Data Analysis, Third Edition* (CRC Press, Nov. 1, 2013).

[27]B. Carpenter, A. Gelman, M. D. Hoffman, D. Lee, B. Goodrich, M. Betancourt, M. Brubaker, J. Guo, P. Li, and A. Riddell, "Stan: a probabilistic programming language", Journal of statistical software **76** (2017).

[28]M. Kay, T. Kola, J. R. Hullman, and S. A. Munson, "When (ish) is my bus? user-centered visualizations of uncertainty in everyday, mobile predictive systems", in Proceedings of the 2016 chi conference on human factors in computing systems (2016), pp. 5092–5103.

[29]A. W. H. Chin, J. T. S. Chu, M. R. A. Perera, K. P. Y. Hui, H.-L. Yen, M. C. W. Chan, M. Peiris, and L. L. M. Poon, "Stability of sars-cov-2 in different environmental conditions", The Lancet Microbe (2020).

[30]W. Yang and L. C. Marr, "Mechanisms by which ambient humidity may affect viruses in aerosols", Applied and Environmental Microbiology **78**, 6781–6788 (2012).

[31]W. Yang, S. Elankumaran, and L. C. Marr, "Relationship between humidity and influenza a viability in droplets and implications for influenza's seasonality", PLoS ONE **7** (2012).

[32]J. Posada, J. Redrow, and I. Celik, "A mathematical model for predicting the viability of airborne viruses", Journal of Virological Methods **164**, 88–95 (2010).

[33]E. Lofgren, N. H. Fefferman, Y. N. Naumov, J. Gorski, and E. N. Naumova, "Influenza seasonality: underlying causes and modeling theories", Journal of Virology **81**, 5429–5436 (2007).

[34]J. E. Benbough, "Some factors affecting the survival of airborne viruses", The Journal of General Virology **10**, 209–220 (1971).

[35]T. N. Estep, M. K. Bechtel, T. J. Miller, and A. Bagdasarian, "Virus inactivation in hemoglobin solutions by heat", Biomaterials, Artificial Cells and Artificial Organs **16**, 129–134 (1988).

[36]S. Gertsman, A. Agarwal, K. O'Hearn, R. J. Webster, A. Tsampalieros, N. Barrowman, M. Sampson, L. Sikora, E. Staykov, R. Ng, and et al., "Microwave- and heat-based decontamination of n95 filtering facepiece respirators: a systematic review", Open Science Framewor (2020).

Supplementary Information

Bayesian estimation models

Model notation

In the model notation that follows, the symbol $\sim$ denotes that a random variable is distributed according to the given distribution. Normal distributions are parametrized as:

$$\text{Normal}(\text{mean}, \text{standard deviation})$$

Positive-constrained normal distributions ("Half-Normal") are parametrized as:

$$\text{Half-Normal}(\text{mode}, \text{standard deviation})$$

Titer inference

We inferred individual titers directly from titration well data using a Poisson single-hit model. We assigned a weakly informative Normal prior to the $\log_{10}$ titers v_i (v_i is the titer for sample i measured in $\log_{10}\text{TCID}_{50}$/0.1mL, since wells were inoculated with 0.1mL):

$$v_i \sim \text{Normal}(2.5, 3) \tag{1}$$

We then modeled individual positive and negative wells for sample i according to a Poisson single-hit model [25]. That is, the number of virions that successfully infect cells within a given well is Poisson distributed with mean:

$$\ln(2)10^{v_i} \tag{2}$$

The value of the mean derives from the fact that our units are TCID_{50}; the probability of a positive well at $v_i = 0$, i.e. 1 TCID_{50}, is equal to $1 - \exp(-\ln(2) \times 1) = 0.5$.

Let Y_{idk} be a binary variable indicating whether the k^{th} well at dilution factor d (where d expressed as $\log_{10}$ dilution factor) for sample i was positive (so $Y_{idk} = 1$ if that well was positive and 0 if it was negative). Under a single-hit process, a well will be positive as long as at least one virion successfully infects a cell.

It follows from equation 2 that the conditional probability of observing $Y_{idk} = 1$ given a true underlying $\log_{10}$ titer v_i is given by:

$$\mathcal{L}(Y_{idk} = 1 \mid v_i) = 1 - \exp(-\ln(2) \times 10^{(v_i - d)}) \tag{3}$$

This is simply the probability that a Poisson random variable with mean $10^{(v_i - d)}$ is greater than 0, and $v_i - d$ is the expected concentration of virions, measured in $\log_{10}\text{TCID}_{50}$, in

the dilute sample. Similarly, the conditional probability of observing $Y_{idk} = 0$ given a true underlying $\log_{10}$ titer v_i is:

$$\mathcal{L}(Y_{idk} = 0 \mid v_i) = \exp(-\ln(2) \times 10^{(v_i - d)}) \tag{4}$$

which is the probability that the Poisson random with variable is equal to 0.

This gives us our likelihood function, assuming independence of outcomes across wells. Our inoculated doses were of volume 0.1 mL, so we incremented inferred titers by 1 to convert to units of $\log_{10}\text{TCID}_{50}$/mL.

Virus inactivation regression

Duration of virus of detectability depends not only on environmental conditions and treatment method but also initial inoculum and sampling noise. We therefore estimated the exponential decay rates of viable virus (and thus virus half-lives) using a Bayesian regression analogous to that used in [5, 11]. This modeling approach allowed us to account for differences in initial inoculum levels across samples as well as other sources of experimental noise. The model yields estimates of posterior distributions of viral decay rates and half-lives in the various experimental conditions – that is, estimates of the range of plausible values for these parameters given our data, with an estimate of the overall uncertainty [26].

Our data consist of four different experimental conditions corresponding to four heat-treatment procedures, all at 70°C: (1) an uncovered plate of wells in a dry oven, (2) a covered plate in the oven, (3) a set of closed vials in the oven, and (4) set of closed vials in a heat block.

For each treatment, we took three samples per time point at multiple time-points.

We model each sample j for experimental condition i as starting with some true initial $\log_{10}$ titer: v_{ij0}. At the time t_{ij} that it is sampled, it has titer v_{ij}.

We assume that viruses in experimental condition i decay exponentially at a rate λ_i over time. It follows that:

$$v_{ij} = v_{ij0} - \lambda_i t_{ij} \tag{5}$$

We use the direct-from-well data likelihood function described above, except that now instead of titers we estimate λ_i under the assumptions that our observed well data Y_{idk} reflect the titers v_{ij}.

We assume that each experiment i has a mean initial $\log_{10}$ titer $\bar{v}_{i0}$. We model the individual v_{ij0} as normally distributed about $\bar{v}_{i0}$ with an estimated, experiment-specific standard deviation σ_i:

$$v_{ij0} \sim \text{Normal}(\bar{v}_{i0}, \sigma_i) \tag{6}$$

Regression prior distributions

We place a Normal prior on the mean initial $\log_{10}$ titers $\bar{v}_{i0}$ that reflects the known inocula.

$$\bar{v}_{i0} \sim \text{Normal}(4.5, 0.5) \tag{7}$$

We place a Half-Normal prior on the standard deviations σ_i that allows for potentially large variation (1 log) variation about the experiment mean, as well as for less variation:

$$\sigma_i \sim \text{Half} - \text{Normal}(0, 0.25) \tag{8}$$

To encode prior information about the decay rate in an interpretable way, we place a Normal prior on the log half-lives $\ln(h_i)$, where $h_i = \frac{\ln(2)}{\lambda_i}$:

$$\ln(h_i) \sim \text{Normal}(\ln(0.5), 2) \tag{9}$$

Predictive checks

We assessed the appropriateness of prior distribution choices using prior predictive checks and assessed goodness of fit for the estimated model using posterior predictive checks. The resultant checks are shown below.

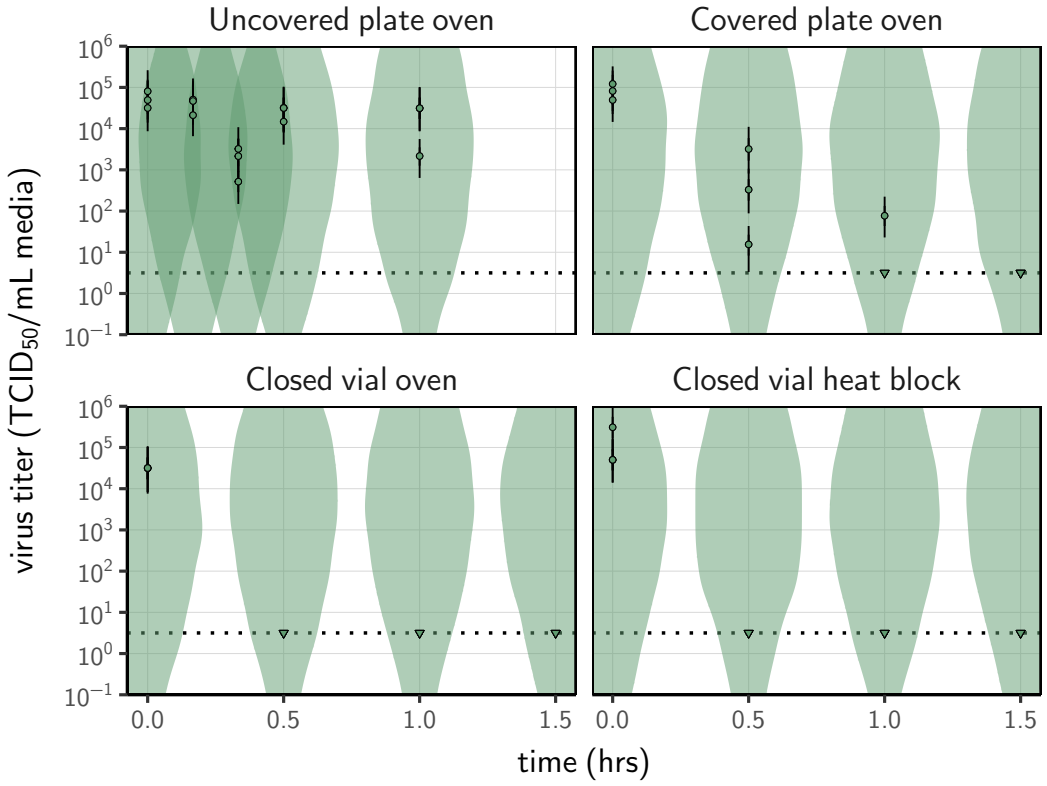

Figure 3. Titer estimation prior check. Violin plots show distribution of simulated titers sampled from the prior predictive distribution. Points show estimated titers for each collected sample; vertical bar shows a 95% credible interval. Time-points with no positive wells for any replicate are plotted as triangles at the approximate single-replicate detection limit of the assay (LOD; denoted by a black dotted line at $10^{0.5}$ $TCID_{50}$/mL media) to indicate that a range of sub-LOD values are plausible. Wide coverage of violins relative to datapoints show that priors are agnostic over the titer values of interest.

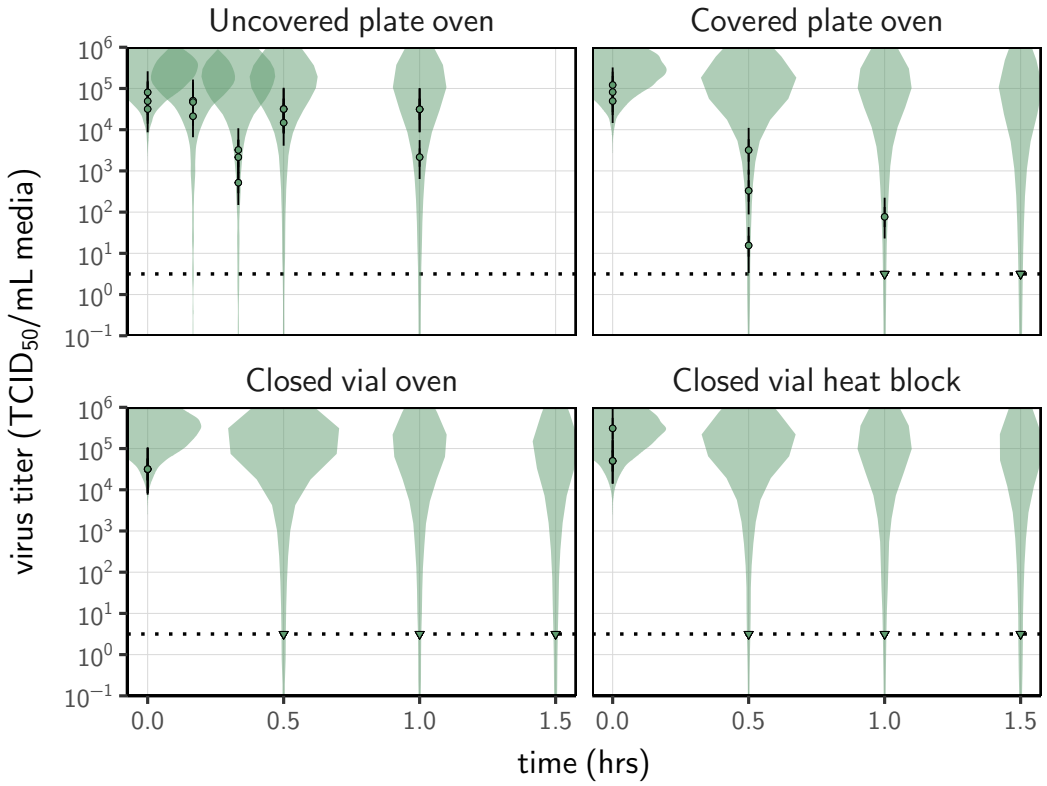

Figure 4. Prior predictive check for regression model. Violin plots show distribution of simulated titers sampled from the prior predictive distribution. Points show estimated titers for each collected sample; vertical bar shows a 95% credible interval. Time-points with no positive wells for any replicate are plotted as triangles at the approximate single-replicate detection LOD (denoted by a black dotted line at $10^{0.5}$ $TCID_{50}$/mL media) to indicate that a range of sub-LOD values are plausible. Wide coverage of violins relative to datapoints show that priors are agnostic over the titer values of interest, and that the priors regard both fast and slow decay rates as possible.

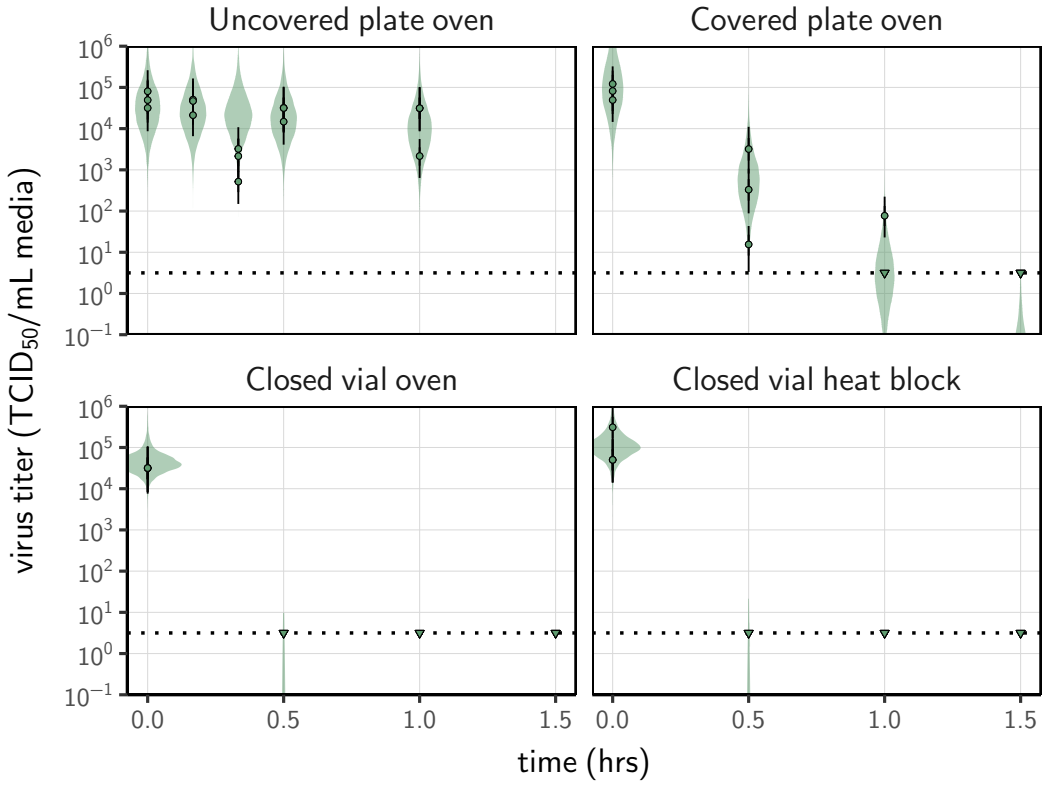

Figure 5. Posterior predictive check for regression model. Violin plots show distribution of simulated titers sampled from the prior predictive distribution. Points show estimated titers for each collected sample; vertical bar shows a 95% credible interval. Time-points with no positive wells for any replicate are plotted as triangles at the approximate single-replicate detection LOD (denoted by a black dotted line at $10^{0.5}$ $TCID_{50}$/mL media) to indicate that a range of sub-LOD values are plausible. Tight fit correspondence between distribution of posterior simulated titers and estimated titers suggests the model fits the data well.